Title: The role of lysine^{100} in the binding of acetylcoenzyme A to human arylamine N-acetyltransferase 1: Implications for other acetyltransferases

Author: Rodney F. Minchin Neville J. Butcher

PII: S0006-2952(15)00084-2
DOI: http://dx.doi.org/doi:10.1016/j.bcp.2015.01.015
Reference: BCP 12184

To appear in: *BCP*

Received date: 12-1-2015
Revised date: 27-1-2015
Accepted date: 28-1-2015

Please cite this article as: Minchin RF, Butcher NJ, The role of lysine^{100} in the binding of acetylcoenzyme A to human arylamine N-acetyltransferase 1: implications for other acetyltransferases, *Biochemical Pharmacology* (2015), http://dx.doi.org/10.1016/j.bcp.2015.01.015

*Graphical Abstract (for review)

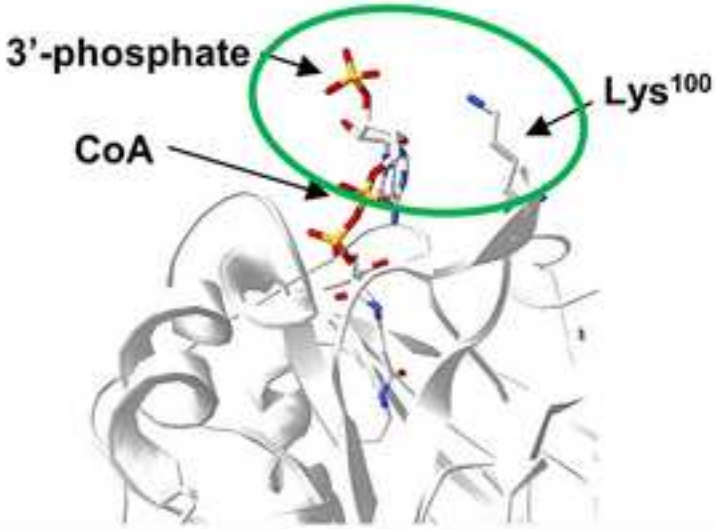

The 3'-phosphoanion of acetylcoenzyme A interacts with Lys^{100} of NAT1 forming a stable complex. Compounds that bind to Lys^{100} may be effective inhibitors of the enzyme.

The role of lysine^{100} in the binding of acetylcoenzyme A to human arylamine N-acetyltransferase 1: implications for other acetyltransferases

Rodney F. Minchin* and Neville J. Butcher

Laboratory for Molecular and Cellular Pharmacology, School of Biomedical Sciences, University of Queensland, Brisbane, Queensland, Australia, 4072.

*Correspondence: r.minchin@uq.edu.au

ABSTRACT

The arylamine N-acetyltransferases (NATs) catalyze the acetylation of aromatic and heterocyclic amines as well as hydrazines. All proteins in this family of enzymes utilize acetyl coenzyme A (AcCoA) as an acetyl donor, which initially binds to the enzyme and transfers an acetyl group to an active site cysteine. Here, we have investigated the role of a highly conserved amino acid (Lys$^{100)}$ in the enzymatic activity of human NAT1. Mutation of Lys^{100} to either a glutamine or a leucine significantly increased the Ka for AcCoA without changing the Kb for the acetyl acceptor p-aminobenzoic acid. In addition, substrate inhibition was more marked with the mutant enzymes. Steady state kinetic analyzes suggested that mutation of Lys^{100} to either leucine or glutamine resulted in a less stable enzyme-cofactor complex, which was not seen with a positively charged arginine at this position. When p-nitrophenylacetate was used as acetyl donor, no differences were seen between the wild-type and mutant enzymes because p-nitrophenylacetate is too small to interact with Lys^{100} when bound to the active site. Using 3'-dephospho-AcCoA as the acetyl donor, kinetic data confirmed that Ly^{100} interacts with the 3'-phosphoanion to stabilise the enzyme-cofactor complex. Mutation of Lys^{100} decreases the

affinity of AcCoA for the protein and increases the rate of CoA release. Crystal structures of several other unrelated acetyltransferases show a lysine or arginine residue within 3 Å of the 3'-phosphoanion of AcCoA, suggesting that this mechanism for stabilizing the complex by the formation of a salt bridge may be widely applicable in nature.

Keywords: Arylamine N-acetyltransferase, kinetics, mutagenesis, AcetylCoenzyme A, lysine

1. Introduction

Acetyltransferases are a diverse superfamily of enzymes involved in the modification of small drug molecules, xenobiotics, peptide and proteins. They are found in all prokaryotic and eukaryotic species studied to date and are essential for numerous intracellular pathways. While the acetyl acceptor varies considerably between different acetyltransferases, they all share a common acetyl donor, acetylcoenzyme A (AcCoA). The arylamine *N*-acetyltransferases (NATs; EC 2.3.1.5) are xenobiotic metabolizing enzymes widely distributed in the animal kingdom [1]. They are distinguished by the presence of a conserved catalytic triad that prefers aromatic amine and hydrazine substrates [2]. In humans, there are 2 NATs (NAT1 and NAT2) and their crystal structure and catalytic function have been described in detail [3-6]. Both NAT1 and NAT2 are genetically polymorphic, which impacts on the pharmacology of many therapeutic agents that are metabolized by these enzymes [7]. Moreover, recent studies have shown a relationship between NAT1 and cancer cell proliferation and survival suggesting that this protein is a potential drug target [7, 8]. There have also been a number of reports on the development of small molecule inhibitors for human and non-human NATs [9-12].

The NATs catalyze the acetylation of small molecules via a double displacement or ping pong bi bi reaction [13]. An in-depth understanding of the catalytic mechanism of the mammalian NAT's was provided by Wang *et al* who examined the acetylation of various substrates by the hamster homolog of NAT1 using Bronsted plot analyses, kinetic solvent isotope effects and pH-dependence studies [14, 15]. This work showed that the formation of a thiolate-imidazolium ion pair by Cys^{68} and His^{107} was essential for enzymatic function. The acetyl donor,

which binds first, is orientated by several amino acids that line the cavity of the active site. This is true for both mammalian and bacterial NAT [6, 16]. In human NAT2, the amino acids reside in the β2 and β3 domains, which extent from amino acids 93-104 (FYIPPVNKYSTG), and in the α9 domain at amino acids 208-217 (YLQTSPTSF). These regions are highly conserved across mammalian NATs suggesting a common mechanism for AcCoA binding (Figure 1A).

The outer surface of the active site pocket for both human NAT1 and NAT2 contains a conserved lysine (Lys^{100}). The crystal structure of the NAT2-CoA binary complex shows that Lys^{100} is in close proximity to the 3'-phosphoanion of CoA (RCSB Protein Data Bank 2PFR) [6]. A similar arrangement is seen with the ε-amino group of Lys^{248} in the NAT homolog from *Bacillus anthracis* [16]. In the mammalian NATs, K^{100} is located on the flexible β2-β3 loop, which shifts towards the center of the active site cleft upon CoA binding [6]. This suggests that Lys^{100} may be involved in the interaction of the acetyl donor with the NATs.

NAT1 is widely distributed in the body and is responsible for metabolism of many therapeutic and carcinogenic compounds [17]. The crystal structure of NAT1 has been reported and it retains the same structural features as other mammalian NATs [6]. Site-directed mutagenesis has been extensively used with both NAT1 and NAT2 to discover critical amino acids involved in the reaction mechanism [15, 18, 19], substrate specificity [20] and stability [21, 22]. Because recent studies have suggested that NAT1 may be a novel drug target [7, 8], insight into how substrates interact with the protein provides important information for the design and development of small molecule inhibitors. In the present study, we have investigated the role of the conserved K^{100} in the acetylation of substrates by NAT1 using steady state enzyme kinetics of wild-type and K^{100} mutants that vary in the charge of their side chain. In addition, different acetyl donors have been studied with the view of establishing whether K^{100} influences their interaction with the enzyme.

2. Materials and Methods

2.1. Materials.

p-Aminobenzoic acid, acetylcoenzyme a, de-phospho-coenzyme A and acetic anhydride were obtained from Sigma Aldrich (St Louis, USA). RPMI1640, serum and LipofectAMINE 2000 were obtained from Life Technologies (Victoria, Australia). Primers were purchased from GeneWorks (South Australia, Australia). All other chemicals were of analytical grade.

2.2 Cells Culture.

HeLa cells were obtained from the American Type Culture Collection (Manassas, VA) and cultured in RPMI-1640 medium supplemented with 5% fetal bovine serum at 37^{o}C in a humidified 5% CO2 atmosphere.

2.3. Mutagenesis.

Lys^{100} was mutated to either a glutamine, leucine or arginine residue using the GENEART site-directed mutagenesis system (Life Technologies, Vic, Australia) as described in the manufacturer's protocol. Wild-type FLAG-tagged human NAT1 [22] was used as template with the following primers; K^{100}Q FP, 5'-agcactccagccaaacaatacagcactggcatg-3', K^{100}Q RP, 5'-catgccagtgctgtattgtttggctggactgct-3', K^{100}L FP, 5'-agcactccagccaaattatacagcactggcatg-'3, K^{100}L RP, 5'- catgccagtgctgtaaatttttggctggactgct -3', K^{100}R FP, 5'-agcactccagccaaaagatacagcactggcatg-3', K^{100}R RP,5'- catgccagtgctgtatctttttggctggactgct -3'. Clones were verified by sequencing.

2.4. Transient Transfection and Protein Expression.

Cells were seeded at a density of 0.8 × 10^{6} cells/well in 6-well plates and allowed to adhere overnight. They were then transiently transfected with 4 μg plasmid DNA using LipofectAMINE 2000 according to the manufacturer's instructions and incubated overnight. Cells were washed twice with cold PBS and then scraped into 0.6 ml of 20 mM Tris/1 mM EDTA buffer (pH 7.4) containing 1 mM dithiothreitol and disrupted on ice by sonication. Cell lysates were centrifuged at 16,000 × g for 10 min (4^{o}C) and the supernatants retained for FLAG Western blot and NAT1 activity assays.

2.5. NAT1 Assay.

NAT1 activity was assayed using *p*-aminobenzoic acid (PABA) as substrate and either AcCoA, dephospho-AcCoA, or *p*-nitrophenylacetate (*p*NPA) as cofactor. N-acetyl-PABA was measured by high performance liquid chromatography as previously described.[23] Kinetic parameters for PABA were determined using 1100 µM cofactor and 0 to 1200 µM PABA. For the determination of cofactor kinetic parameters, 420 µM PABA was used with 0 to 1200 µM cofactor. All reactions were performed under linear conditions with respect to substrate and protein. NAT1 activities were normalized for protein expression using FLAG Western blots of each cell lysate.

2.6. Synthesis of Dephospho-AcCoA.

Acetyl-3'-dephospho-coenzyme A was synthesized as previously described.[22] Briefly, 2.3 mg 3'-dephospho-coenzyme A (Sigma-Aldrich) was dissolved in 200 µl NH_4OH. Acetic anhydride (16 µl) was added on ice over 30 min with shaking. The solution was then freeze dried to remove the solvent and the excess acetic acid. The acetyl-3'-dephospho-coenzyme A was dissolved in water and analyzed by HPLC before use.

2.7. Data Analysis.

Steady state kinetics were analyzed based on the reaction mechanism shown in Scheme 1, which describes a double displacement or ping pong bi bi reaction with substrate inhibition. The initial velocity (v) was described by:

$$v = \frac{V_{max}.A.B}{K_a.B.\left(1+\frac{B}{K_i}\right)+K_b.A+A.B} \quad (1)$$

where Vmax = maximum velocity, A = acetyl donor concentration (AcCoA or *p*NPA), B = acetyl acceptor concentration (PABA), K_a = kinetic constant for the acetyl donor, K_b = kinetic constant for the acetyl acceptor (PABA) and K_i = substrate inhibition constant. For experiments

where the acetyl acceptor was varied and the acetyl donor was constant, equation 1 was rearranged to:

$$v = \frac{V_{max} \cdot B}{K_b + B\left(1 + \frac{K_a}{A}\left[1 + \frac{B}{K_i}\right]\right)} \quad (2)$$

All kinetic parameters were estimated by nonlinear least squares regression using GraphPad Prism 6 (GraphPad Software, La Jolla, USA) and comparisons were performed using a Student's *t*-test. Convergence was confirmed by initiating the iterative process from at least 3 independent initial estimates. Kinetic parameters were compared by one way analysis of variance.

2.8. Crystal structure analysis.

All crystal structure coordinates were obtained from the Brookhaven protein database and were visualized using Swiss PDB Viewer Ver 4.0.1 (Swiss Institute of Bioinformatics). Reported distances were calculated using the same software.

3. Results

3.1. Steady state kinetics of PABA acetylation by NAT1.

The mechanism for the acetylation of substrates by NAT1 is shown in Figure 2A and comprises 2 sequential reactions. AcCoA initially binds to the enzyme and acetylates Cys[68]. Following release of CoA, the acetyl acceptor interacts with the acetylated enzyme to form product. The second reaction is independent of the acetyl donor as it leaves the enzyme before the acetyl acceptor binds. However, as with many ping pong bi bi reactions, competition between acetyl donor and acetyl acceptor for the unacetylated enzyme can occur. This results in substrate-dependent inhibition at high concentrations, as has been described for the human NATs [23]. Initially, we examined the kinetics of NAT1 acetylation using the different acetyl donors, AcCoA and pNPA. Both compounds readily support the first half of the reaction but pNPA is much smaller and lacks the phosphor-ADP and pantothenic groups of AcCoA that interact with the β2 and β3 domains of the enzyme (Figure 2C). For pNPA, the reaction kinetics are slightly different to that for AcCoA because pNPA reportedly does not form a Michaelis complex [14].

Equation 1 and 2 still described the relationship between concentrations and reaction velocities. However, the interpretation of K_a is somewhat different. For AcCoA, $K_a = [k_4*(k_{-1} + k_2)]/[k_1(k_2 + k_4)]$ whereas for pNPA, $K_a = k_4/k_2$ [14].

Initially, the kinetics of PABA acetylation was studied in wild-type enzyme ectopically expressed in HeLa cells to ensure post-translational modification of the enzyme. The initial rates of reaction using pNPA and AcCoA as acetyl donors are shown in Figure 3A. Substrate inhibition was evident for both donors, although this was seen at a lower substrate concentration with pNPA. To determine the kinetic parameters for both the acetyl donors and the acetyl acceptor, equation 2 was simultaneously fitted to the data with the assumption that K_b and K_i are independent of the acetyl donor used. The resulting kinetic parameters are shown in Table 1 (rows 1 and 4). For pNPA, K_a was almost 10 times that seen for AcCoA. In addition, V_{max} was almost 4 fold greater for pNPA. V_{max} is a measure of the rate of product formation and, for a double displacement mechanism, it is equal to the product of [S●AcE] and k_4 (Figure 2A & B). Since k_4 is independent of the acetyl donor, the difference in V_{max} indicates that the steady state [S●AcE] was higher for pNPA.

3.2. Effect of Lys^{100} mutations on NAT1 kinetics.

To examine the role of Lys^{100} in NAT1 catalytic activity, the amino acid was mutated to either a glutamine ($K^{100}Q$) or a leucine ($K^{100}L$). With pNPA as the acetyl donor, PABA acetylation was similar for both the wild-type and the mutated forms of the enzyme (Figure 3B). The estimated steady state kinetic parameters are shown in Table 1 (rows 1-3). The lack of any effect following mutation indicates that Lys^{100} is not involved in the binding of pNPA to the enzyme, which is consistent with its location deep within the catalytic pocket away from the β2 and β3 domains. In addition, the results suggest Lys^{100} does not influence the binding of the acetyl acceptor (PABA) to the enzyme. Using the kinetic parameter estimates in Table 1, inhibition by PABA at the different concentrations was calculated and is plotted in Figure 3C. The data show that mutation of Lys^{100} did not affect the competition between pNPA and PABA for the unacetylated enzyme. The lack of any change in the estimates for the PABA inhibition constant K_i is in agreement with this conclusion.

When AcCoA was used as the acetyl donor, the reaction kinetics were very different between the mutant and the wild-type enzymes (Figure 3D). Table 1 (rows 4-6) shows a significant increase ($p<0.05$) in the acetyl donor kinetic constant (K_a) from 0.68 mM for the wild-type enzyme to 8-10 mM for the $K^{100}Q$ and $K^{100}L$ mutant enzymes. Moreover, the extent of substrate inhibition was much greater for the mutant enzymes (Figure 3E). This suggests that the affinity of AcCoA for the enzyme was decreased since K_i did not change (Table 1).

To test whether the charge at K^{100} affected NAT1 activity, the lysine was mutated to an arginine ($K^{100}R$) and the resulting steady state velocities are shown in Figure 3D. The K_a for AcCoA was similar to that for the wild-type enzyme (Table 1). However, the $K^{100}R$ mutant did not fully recover activity as the V_{max} for the reaction was significantly less ($p<0.05$) than that of the wild-type enzyme. Nevertheless, these results suggest that the charge of the amino acid at position 100 influences the affinity of AcCoA for the enzyme.

To confirm the effects of K^{100} mutation on the kinetics of AcCoA, steady state reaction velocities were determined using a constant PABA concentration (420 μM) and increasing AcCoA concentrations for both the wild-type and mutant enzymes (Figure 3F). Over the concentration range of 0 to 1.2 mM, saturation of the wild-type and $K^{100}R$ enzymes was seen. This is consistent with the K_a less than 1 mM shown in Table 1. By contrast, activity was significantly less and no saturation was seen with the $K^{100}L$ and $K^{100}Q$ enzymes, in agreement with the increased K_a for these enzymes. The parameter V_{max}/K_a is the rate constant for the association and formation of a productive complex (acetylated enzyme intermediate) by the acetyl donor [24]. For pNPA, V_{max}/K_a was independent of Lys^{100} (Table 1). By contrast, for AcCoA, V_{max}/K_a decreased more than 4 fold when Lys^{100} was replaced with either a glutamine or a leucine. This indicates that the mutated enzymes do not form a productive complex with AcCoA to the same degree as the wild-type enzyme.

3.3. Effect of the 3'-phosphoanion of AcCoA on NAT1 kinetics.

Because the crystal structure of CoA bound to NAT2 suggested that K^{100} might interact with the 3'-phosphoanion of the acetyl donor, 3'-dephosphorylated AcCoA (dephospho-AcCoA) was synthesized and used as the acetyl donor (Figure 2C). The steady state velocities are shown in Figure4. For the wild-type and $K^{100}R$ enzymes, K_a was high (~15 mM), similar to that seen for

AcCoA with the $K^{100}L$ and $K^{100}Q$ enzymes (Table 1). These data suggest that removal of the positive charge at position 100 of NAT1 or removal of the negative 3'-phosphoanion from the acetyl donor had the same effects on enzyme kinetics. Surprisingly, the K_a for dephospho-AcCoA increased even further when the $K^{100}L$ and $K^{100}Q$ enzymes were examined (Table 1), resulting in a further decrease in activity for PABA acetylation (Figure 4). Thus, removal of both the positively charged amino acid at position 100 and the negatively charged 3'-phosphoanion on AcCoA affected enzyme activity much greater than each of the individual changes. This is shown in the estimates for V_{max}/K_a. For the wild-type enzyme, V_{max}/K_a decreased from 2955 $\pm$ 345 for AcCoA as acetyl donor to 405 $\pm$ 45 for dephospho-AcCoA as acetyl donor. Moreover, this value decreased further to ~ 200 when Lys^{100} was replaced by either glutamine or leucine. However, unlike that seen with AcCoA, there was no difference in activity between the wild-type enzyme and the $K^{100}R$ mutant when dephospho-AcCoA was used as the acetyl donor (Table 1 and Figure 4).

3.4. Lysine-CoA interactions in other arylamine N-acetyltransferases.

We examined the structures of several other arylamine N-acetyltransferase-CoA complexes available in public databanks to determine whether the binding of the 3'-phosphoanion of AcCoA to a lysine residue was common for this class of emzyme. Figure 5 shows structures for NAT from *Bacillus anthracis* (RCSB Protein Data Bank 3LNB), published by Pluvinage et al ([16], and for NAT from *Mycobacterium marinum* (RCSB Protein Data Bank 2VFC), published by Fullam et al [25]. For *B anthracis*, Lys^{248} is located at the surface of the catalytic pocket and within 3 Å of the 3'phosphoanion of CoA, sufficiently close to form a salt bridge. The crystal structure indicates that Lys^{248} may also interact with the 5'-phosphate as well (Figure 5A). For *M marinum*, the lysine closest to the 3'-phosphoanion of CoA is Lys^{236}, which is within 3.3 Å of the ε-amino group. However, the crystal structure suggests that Lys^{236} does not interact with the 5'phosphoanion. If this were the case, then it could be predicted that the enzyme-AcCoA complex is more stable for *B anthracis* because of the dual interaction of the acetyl donor with Lys^{248}. This should result in a lower K_a for the acetylation reaction. Indeed,

this is the case. Pluvinage et al reported an AcCoA Km_{app} of 50 μM for the *B anthracis* enzyme and approximately 200 μM for the *M marinum* enzyme.

4. Discussion

The arylamine N-acetyltransferases are a family of ancient enzymes found across many prokaryotes and eukaryotes species [1]. They have been associated with a number of human disorders including drug resistance [26, 27], drug hypersensitivity [28, 29], atopic allergic responses [30], and drug-induced liver disease [31]. More recently, the NATs have been proposed as possible small molecule drug targets [7, 8, 32] and an understanding of their structure and catalytic mechanism may provide important leads to designing such targets. In the present study, we have investigated the role of a conserved lysine residue located at the surface of the catalytic pocket of NAT1, and found that this amino acid is important in AcCoA binding to the enzyme. These results suggest that the design of NAT1 inhibitors could include binding to K^{100}. This may increase affinity because K^{100} appears to significantly stabilize the substrate-enzyme complex even when other amino acids in the active site pocket are involved in binding.

Experiments replacing AcCoA with the acetyl donor pNPA support a role for Lys^{100} in the interaction of AcCoA with NAT1. pNPA is much smaller than AcCoA and is unlikely to make contact with Lys^{100} when located in the active site of the enzyme. There were no major differences in the steady-state kinetics of PABA acetylation between the wild-type and mutant proteins when pNPA was used as the acetyl donor. These kinetic data and previously published co-crystal structures of NATs-CoA [6] indicate that Lys^{100} interacts with the 3'-phosphoanion of AcCoA, and this finding was supported by experiments using dephospho-AcCoA.

Analysis of the kinetic constants provides some insight into how Lys^{100} affects AcCoA binding. The lack of any effect of Lys^{100} mutation on enzyme activity with pNPA as acetyl donor indicates that this amino acid does not influence PABA binding to the enzyme or the rate of product release, that is, k_3, k_{-3} or k_4 (Figure 2A). When Lys^{100} was mutated to either a glutamine or a leucine, V_{max} more than doubled (Table 1). V_{max} is proportional to $k_2.k_4/(k_2+k_4)$ [14] and since k_4 was unaffected, Lys^{100} must primarily influence k_2, the rate constant for the release of CoA from the enzyme. An increase in k_2 will also lead to an increase in the steady state concentration of the intermediates Ac-E, which would increase the rate of acetyl acceptor

binding to the intermediate (Figure 2A). However, the data do not exclude the possibility that Lys^{100} is also involved in the association and/or dissociation of AcCoA (that is, k_1 and k_{-1}). Figure 3E indicates that PABA competes more effectively with AcCoA for the $K^{100}Q$ and $K^{100}L$ proteins compared to the wild-type enzyme. Since the binding of PABA to the enzyme was not influenced by either of these mutations, the data indicate that the affinity of AcCoA for NAT1 decreased when the charge at position 100 was changed to a non-positive amino acid. The overall outcome of modifying Lys^{100} is a less efficient first half of the reaction (due to a deceased rate of productive interaction between the enzyme and AcCoA) and a more efficient second half of the reaction (due to a faster release of CoA and a higher steady state concentration of the Ac-E intermediate). This conclusion was supported by the experiment in Figure 3E where AcCoA concentration was varied, which showed an increase in K_a. For AcCoA, K_a is a function of k_1, k_{-1}, k_2 and k_4 (see above and [14]). Since k_4 was unaffected by mutation of K^{100}, the increase in K_a suggests a change in k_1, k_{-1} or k_2. Each of these parameters are involved in AcCoA binding and/or the initial acetylation of the active site cysteine.

Removal of the 3'-phosphoanion from AcCoA produced the expected changes in PABA kinetics that mimicked removal of the positive charge at Lys^{100}. However, somewhat unexpectedly, the steady state kinetics for PABA acetylation by the $K^{100}Q$ and $K^{100}L$ mutants showed an even larger increase in K_a to ~ 28 mM. The reason for this is currently unknown but suggests that Lys^{100} may interact with AcCoA in addition to the 3'-phosphoanion. The crystal structure of NAT from *B anthracis* suggests Lys^{248} can simultaneously interact with the 3'-phosphoanion and the 5'-phosphoanion of CoA (Figure 5A), but this is unknown for NAT1.

The interaction of quaternary amines with phosphates has been shown to be a highly stable non-covalent bond [33] so their presence in proteins complexed with small molecule phosphates is expected. The crystal structures of several acetyltransferases unrelated to the NATs also show lysine interactions with CoA. For human choline acetyltransferase, two lysines stabilize the enzyme-CoA complex [34]. Lys^{407} engages with the 3'-phosphoanion while Lys^{403} interacts with the 5'-phosphoanion. Similarly, Lys^{192} in dopamine acetyltransferase from *D. melanogaster* reportedly forms a salt bridge with the 3'-phosphoanion of CoA [35]. There are several other AcCoA-dependent enzymes including GNAT [36], tubulin acetyltransferase [37] and carnitine acetyltransferase[38] where a protein-CoA co-crystal shows the ε-amino group of a

lysine located at a distance from the 3'-phosphoanion that would support the formation of a salt bridge (Figure 6). By contrast, there are several acetyltransferases where the guanidine side chain of an arginine is positioned within 3 Å of the 3'-phosphoanion of bound CoA. These include spermine-spermidine acetyltransferase (Arg^{142} and Arg^{143}) [39] and serotonin acetyltransferases (Arg^{170}) [40]. Both arginine and lysine residues readily undergo post-translational modification, including methylation, acetylation sumoylation and ubiquitination, which would be a novel mechanism for regulating acetyltransferase activity by altering AcCoA binding. However, there currently is scant evidence for post-translational modification of the NATs. An exception is a recent study by Zhang et al, who demonstrated acetylation of 2 lysine residues in NhoA, a N-hydroxyarylamine O-acetyltransferase from *E. coli* [41]. However, it is unknown if either of these lysines interact with AcCoA. We are currently investigating whether Lys^{100} in NAT1 undergoes modification and, if so, whether these changes affect enzyme function.

Acknowledgements

This work was funded by the National Health and Medical Research Council of Australia (Project grant number 1024769).

Competing financial Interests: The authors declare no competing financial interests exist.

References

[1] Sim E, Walters K, Boukouvala S. Arylamine N-acetyltransferases: from structure to function. Drug Metab Rev. 2008;40:479-510.

[2] Sandy J, Mushtaq A, Holton SJ, Schartau P, Noble ME, Sim E. Investigation of the catalytic triad of arylamine N-acetyltransferases: essential residues required for acetyl transfer to arylamines. Biochem J. 2005;390:115-23.

[3] Rodrigues-Lima F, Delomenie C, Goodfellow GH, Grant DM, Dupret JM. Homology modelling and structural analysis of human arylamine N-acetyltransferase NAT1: evidence for the conservation of a cysteine protease catalytic domain and an active-site loop. Biochem J. 2001;356:327-34.

[4] Rodrigues-Lima F, Dupret JM. 3D model of human arylamine N-acetyltransferase 2: structural basis of the slow acetylator phenotype of the R64Q variant and analysis of the active-site loop. Biochem Biophys Res Commun. 2002;291:116-23.

[5] Walraven JM, Trent JO, Hein DW. Computational and experimental analyses of mammalian arylamine N-acetyltransferase structure and function. Drug Metab Dispos. 2007;35:1001-7.

[6] Wu H, Dombrovsky L, Tempel W, Martin F, Loppnau P, Goodfellow GH, et al. Structural basis of substrate-binding specificity of human arylamine N-acetyltransferases. J Biol Chem. 2007;282:30189-97.

[7] Butcher NJ, Minchin RF. Arylamine N-acetyltransferase 1: a novel drug target in cancer development. Pharmacol Rev. 2012;64:147-65.

[8] Rodrigues-Lima F, Dairou J, Busi F, Dupret JM. Human arylamine N-acetyltransferase 1: a drug-metabolizing enzyme and a drug target? Curr Drug Targets. 2010;11:759-66.

[9] Abuhammad A, Fullam E, Lowe ED, Staunton D, Kawamura A, Westwood IM, et al. Piperidinols that show anti-tubercular activity as inhibitors of arylamine N-acetyltransferase: an essential enzyme for mycobacterial survival inside macrophages. PLoS One. 2012;7:e52790.

[10] Chowdhury A, Paul P, Choudhury MD. High Throughput Screening of 7-Methylpicene-1,2-Diol as Arylamine N-Acetyltransferase (NAT) Inhibitor to Establish a Isoniazid

Supplement in Anti-Tubercular Therapy. Comb Chem High Throughput Screen. 2013;16:721-5.

[11] Tiang JM, Butcher NJ, Minchin RF. Small molecule inhibition of arylamine N-acetyltransferase Type I inhibits proliferation and invasiveness of MDA-MB-231 breast cancer cells. Biochem Biophys Res Commun. 2010;393:95-100.

[12] Westwood IM, Bhakta S, Russell AJ, Fullam E, Anderton MC, Kawamura A, et al. Identification of arylamine N-acetyltransferase inhibitors as an approach towards novel anti-tuberculars. Protein Cell. 2010;1:82-95.

[13] Kilbane AJ, Petroff T, Weber WW. Kinetics of acetyl CoA: arylamine N-acetyltransferase from rapid and slow acetylator human liver. Drug Metab Dispos. 1991;19:503-7.

[14] Wang H, Liu L, Hanna PE, Wagner CR. Catalytic mechanism of hamster arylamine N-acetyltransferase 2. Biochemistry. 2005;44:11295-306.

[15] Wang H, Vath GM, Gleason KJ, Hanna PE, Wagner CR. Probing the mechanism of hamster arylamine N-acetyltransferase 2 acetylation by active site modification, site-directed mutagenesis, and pre-steady state and steady state kinetic studies. Biochemistry. 2004;43:8234-46.

[16] Pluvinage B, Li de la Sierra-Gallay I, Kubiak X, Xu X, Dairou J, Dupret JM, et al. The Bacillus anthracis arylamine N-acetyltransferase ((BACAN)NAT1) that inactivates sulfamethoxazole, reveals unusual structural features compared with the other NAT isoenzymes. FEBS Lett. 2011;585:3947-52.

[17] Hein DW. Molecular genetics and function of NAT1 and NAT2: role in aromatic amine metabolism and carcinogenesis. Mutation research. 2002;506-507:65-77.

[18] Dupret JM, Grant DM. Site-directed mutagenesis of recombinant human arylamine N-acetyltransferase expressed in Escherichia coli. Evidence for direct involvement of Cys68 in the catalytic mechanism of polymorphic human NAT2. J Biol Chem. 1992;267:7381-5.

[19] Delomenie C, Goodfellow GH, Krishnamoorthy R, Grant DM, Dupret JM. Study of the role of the highly conserved residues Arg9 and Arg64 in the catalytic function of human N-acetyltransferases NAT1 and NAT2 by site-directed mutagenesis. Biochem J. 1997;323 (Pt 1):207-15.

[20] Goodfellow GH, Dupret JM, Grant DM. Identification of amino acids imparting acceptor substrate selectivity to human arylamine acetyltransferases NAT1 and NAT2. Biochem J. 2000;348 Pt 1:159-66.

[21] Butcher NJ, Arulpragasam A, Minchin RF. Proteasomal degradation of N-acetyltransferase 1 is prevented by acetylation of the active site cysteine: a mechanism for the slow acetylator phenotype and substrate-dependent down-regulation. J Biol Chem. 2004;279:22131-7.

[22] Zang Y, Zhao S, Doll MA, States JC, Hein DW. The T341C (Ile114Thr) polymorphism of N-acetyltransferase 2 yields slow acetylator phenotype by enhanced protein degradation. Pharmacogenetics. 2004;14:717-23.

[23] Riddle B, Jencks WP. Acetyl-coenzyme A: arylamine N-acetyltransferase. Role of the acetyl-enzyme intermediate and the effects of substituents on the rate. J Biol Chem. 1971;246:3250-8.

[24] Northrop DB. On the meaning of K-m and V/K in enzyme kinetics. J Chem Educ. 1998;75:1153-7.

[25] Fullam E, Westwood IM, Anderton MC, Lowe ED, Sim E, Noble ME. Divergence of cofactor recognition across evolution: coenzyme A binding in a prokaryotic arylamine N-acetyltransferase. J Mol Biol. 2008;375:178-91.

[26] Sim E, Payton M, Noble M, Minchin R. An update on genetic, structural and functional studies of arylamine N-acetyltransferases in eucaryotes and procaryotes. Human molecular genetics. 2000;9:2435-41.

[27] Adam PJ, Berry J, Loader JA, Tyson KL, Craggs G, Smith P, et al. Arylamine N-acetyltransferase-1 is highly expressed in breast cancers and conveys enhanced growth and resistance to etoposide in vitro. Molecular cancer research : MCR. 2003;1:826-35.

[28] Romano A. Recognising antibacterial hypersensitivity in children. Paediatric drugs. 2000;2:101-12.

[29] Ohtani T, Hiroi A, Sakurane M, Furukawa F. Slow acetylator genotypes as a possible risk factor for infectious mononucleosis-like syndrome induced by salazosulfapyridine. The British journal of dermatology. 2003;148:1035-9.

[30] Zielinska E, Niewiarowski W, Bodalski J, Stanczyk A, Bolanowski W, Rebowski G. Arylamine N-acetyltransferase (NAT2) gene mutations in children with allergic diseases. Clinical pharmacology and therapeutics. 1997;62:635-42.

[31] Huang YS, Chern HD, Su WJ, Wu JC, Lai SL, Yang SY, et al. Polymorphism of the N-acetyltransferase 2 gene as a susceptibility risk factor for antituberculosis drug-induced hepatitis. Hepatology. 2002;35:883-9.

[32] Sim E, Pinter K, Mushtaq A, Upton A, Sandy J, Bhakta S, et al. Arylamine N-acetyltransferases: a pharmacogenomic approach to drug metabolism and endogenous function. Biochemical Society transactions. 2003;31:615-9.

[33] Woods AS, Moyer SC, Jackson SN. Amazing stability of phosphate-quaternary amine interactions. Journal of proteome research. 2008;7:3423-7.

[34] Kim AR, Rylett RJ, Shilton BH. Substrate binding and catalytic mechanism of human choline acetyltransferase. Biochemistry. 2006;45:14621-31.

[35] Cheng KC, Liao JN, Lyu PC. Crystal structure of the dopamine N-acetyltransferase-acetyl-CoA complex provides insights into the catalytic mechanism. Biochem J. 2012;446:395-404.

[36] Majorek KA, Kuhn ML, Chruszcz M, Anderson WF, Minor W. Structural, functional, and inhibition studies of a Gcn5-related N-acetyltransferase (GNAT) superfamily protein PA4794: a new C-terminal lysine protein acetyltransferase from pseudomonas aeruginosa. J Biol Chem. 2013;288:30223-35.

[37] Taschner M, Vetter M, Lorentzen E. Atomic resolution structure of human alpha-tubulin acetyltransferase bound to acetyl-CoA. Proceedings of the National Academy of Sciences of the United States of America. 2012;109:19649-54.

[38] Hsiao YS, Jogl G, Tong L. Crystal structures of murine carnitine acetyltransferase in ternary complexes with its substrates. J Biol Chem. 2006;281:28480-7.

[39] Montemayor EJ, Hoffman DW. The crystal structure of spermidine/spermine N1-acetyltransferase in complex with spermine provides insights into substrate binding and catalysis. Biochemistry. 2008;47:9145-53.

[40] Scheibner KA, De Angelis J, Burley SK, Cole PA. Investigation of the roles of catalytic residues in serotonin N-acetyltransferase. J Biol Chem. 2002;277:18118-26.

[41] Zhang QF, Gu J, Gong P, Wang XD, Tu S, Bi LJ, et al. Reversibly acetylated lysine residues play important roles in the enzymatic activity of Escherichia coli N-hydroxyarylamine O-acetyltransferase. The FEBS journal. 2013;280:1966-79.

492

493

494 **Table 1.**

495 Kinetic parameters for *p*-aminobenzoic acid acetylation by NAT1

Enzyme	Acetyl Donor	V_{max} [a]	K_a (mM)	K_b (mM)	K_i (mM)	V_{max}/K_a
WT	*p*NPA	7540 ± 410	5.81 ± 0.61	0.21 ± 0.01	1.34 ± 0.09	1300 ± 155
$K^{100}Q$	*p*NPA	7065 ± 225	6.05 ± 0.21	0.20 ± 0.06	1.65 ± 0.10	1170 ± 55
$K^{100}L$	*p*NPA	6075 ± 330*	5.27 ± 0.34	0.18 ± 0.12	1.52 ± 0.19	1150 ± 95
WT	AcCoA	2010 ± 109	0.68 ± 0.07	0.21 ± 0.01	1.34 ± 0.09	2955 ± 345
$K^{100}Q$	AcCoA	5910 ± 370**	10.60 ± 0.75**	0.19 ± 0.15	1.48 ± 0.14	560 ± 55**
$K^{100}L$	AcCoA	4840 ± 230**	8.28 ± 0.46**	0.18 ± 0.10	1.54 ± 0.13	585 ± 40**
$K^{100}R$	AcCoA	760 ± 30**	0.67 ± 0.04	0.20 ± 0.10	1.45 ± 0.38	1135 ± 80
WT	d-AcCoA	6145 ± 460	15.2 ± 1.3	0.19 ± 0.02	1.42 ± 0.08	405 ± 45
$K^{100}Q$	d-AcCoA	5885 ± 260	28.8 ±1.4**	0.21 ± 0.02	0.91 ± 0.14	205 ± 15*
$K^{100}L$	d-AcCoA	4860 ± 140	28.1 ± 0.8**	0.13 ± 0.05	1.10 ± 0.11	175 ± 7*
$K^{100}R$	d-AcCoA	6050 ± 250	12.9 ± 0.6	0.27 ± 0.04	1.67 ± 0.31	470 ± 25

496

[a]nmol/min/DU where DU = density units from Western blots.

* $p<0.05$; ** $p<0.01$ compared to respective control (WT) using one-way analysis of variance with Tukey's correction for multiple comparisons.

Figure legends

Figure1. Sequence homology of mammalian NATs in the β2-β3 and α9 region of the protein. Blue underlined letters refer to amino acids identified in the human NAT2 crystal structure that bind specific regions of the AcCoA molecule [6]. The conserved lysine at position 100 is shown in red.

Figure 2. Acetylation of substrate by human NAT1. The double displacement or ping pong bi bi mechanism for the NATs shows acetylation of the active site cysteine by AcCoA followed by the transfer of the acetyl group to the primary amine of the substrate.(A) Reaction mechanism for AcCoA as the acetyl donor, where a Michaelis complex is formed. (B) Reaction mechanism of pNPA as the acetyl donor, where no Michaelis complex is formed [14]. For both reactions, the reversible binding of substrate to the unacetylated enzyme results in substrate inhibition. (C) Structure of the different acetyl donors used in the current study.

Figure 3. Acetylation of PABA by human NAT1. (A) Kinetic curves for wild-type (WT) NAT1 activity with a constant acetyl donor concentration (1100 μM) and increasing acetyl acceptor concentration. (B) Acetylation of PABA by WT, $K^{100}L$ and $K^{100}Q$ NAT1 mutations with pNPA (1100 μM) as the acetyl donor. (C) Calculated substrate inhibition from the data in B at each concentration of PABA. (D) Acetylation of PABA by WT, $K^{100}L$, $K^{100}Q$ and $K^{100}R$ NAT1 mutations with AcCoA (1100 μM) as the acetyl donor. (E) Calculated substrate inhibition from the data in D at each concentration of PABA. (F) Acetylation of PABA by WT, $K^{100}L$, $K^{100}Q$ and $K^{100}R$ NAT1 mutations at a constant PABA concentration (420 μM) and increasing AcCoA concentrations. All data are mean ± s.e.m, n = 3. DU = density units obtained from quantification of Western blots.

Figure 4. Acetylation of PABA by WT, $K^{100}L$, $K^{100}Q$ and $K^{100}R$ NAT1 mutations at a constant concentration (1100 μM) of dephospho-AcCoA as acetyl donor. Data are shown as mean ± s.e.m, n = 3. DU = density units obtained from quantification of Western blots.

Figure 5. Location of lysine residues in bacterial NATs bound with AcCoA. (A) Crystal structure of *Bacillus anthracis* NAT showing the location of Lys^{248} in relation to the 3'-phosphoanion and 5'-phosphoanion groups of AcCoA. Structural coordinates were taken from Brookhaven database (3LNB) after the work of Pluvinage et al ([16]. (B) Crystal structure of *Mycobacterium marinum* NAT showing the location of Lys^{236} in relation to the 3'-phosphoanion of AcCoA. Structural coordinates were obtained from Brookhaven database (2VFC) after the work of Fullam et al [25]. Structures were drawn with Swiss PDB Viewer (4.1), which was also used to calculate distances.

Figure 6. Structural analysis of AcCoA binding to acetyltransferases. Structures showing lysine residues in close proximity to the 3'-phosphoanion of AcCoA. Structural coordinates were obtained from Brookhaven database. Choline acetyltransferase = 2FY5; dopamine acetyltransferase = 3T4E; GNAT = 2I79; tubulin acetyltransferase = 4H6Z; polyamine acetyltransferase = 3QB8; carnitine acetyltransferase = 1NDB. Structures were drawn with Swiss PDB Viewer (4.1), which was also used to calculate distances.

Figure 1

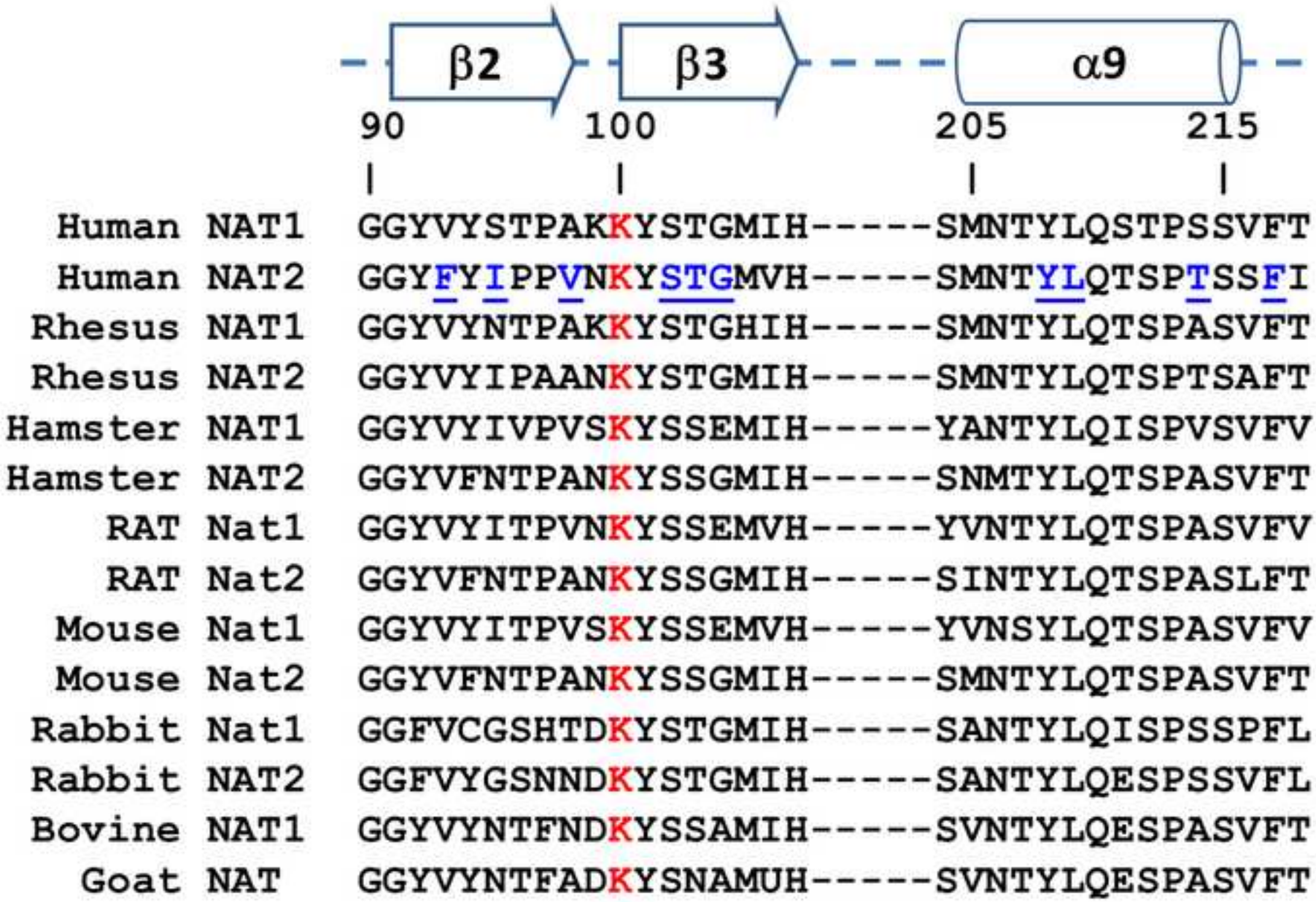
β2
β3
α9
90
100
205
215
Human NAT1 GGYVYSTPAKKYSTGMIH-----SMNTYLQSTPSSVFT
Human NAT2 GGYFYIPPVNKYSTGMVH-----SMNTYLQTSPTSSFI
Rhesus NAT1 GGYVYNTPAKKYSTGHIH-----SMNTYLQTSPASVFT
Rhesus NAT2 GGYVYIPAANKYSTGMIH-----SMNTYLQTSPTSAFT
Hamster NAT1 GGYVYIVPVSKYSSEMIH-----YANTYLQISPVSVFV
Hamster NAT2 GGYVFNTPANKYSSGMIH-----SNMTYLQTSPASVFT
RAT Nat1 GGYVYITPVNKYSSEMVH-----YVNTYLQTSPASVFV
RAT Nat2 GGYVFNTPANKYSSGMIH-----SINTYLQTSPASLFT
Mouse Nat1 GGYVYITPVSKYSSEMVH-----YVNSYLQTSPASVFV
Mouse Nat2 GGYVFNTPANKYSSGMIH-----SMNTYLQTSPASVFT
Rabbit Nat1 GGFVCGSHTDKYSTGMIH-----SANTYLQISPSSPFL
Rabbit NAT2 GGFVYGSNNDKYSTGMIH-----SANTYLQESPSSVFL
Bovine NAT1 GGYVYNTFNDKYSSAMIH-----SVNTYLQESPASVFT
Goat NAT GGYVYNTFADKYSNAMUH-----SVNTYLQESPASVFT

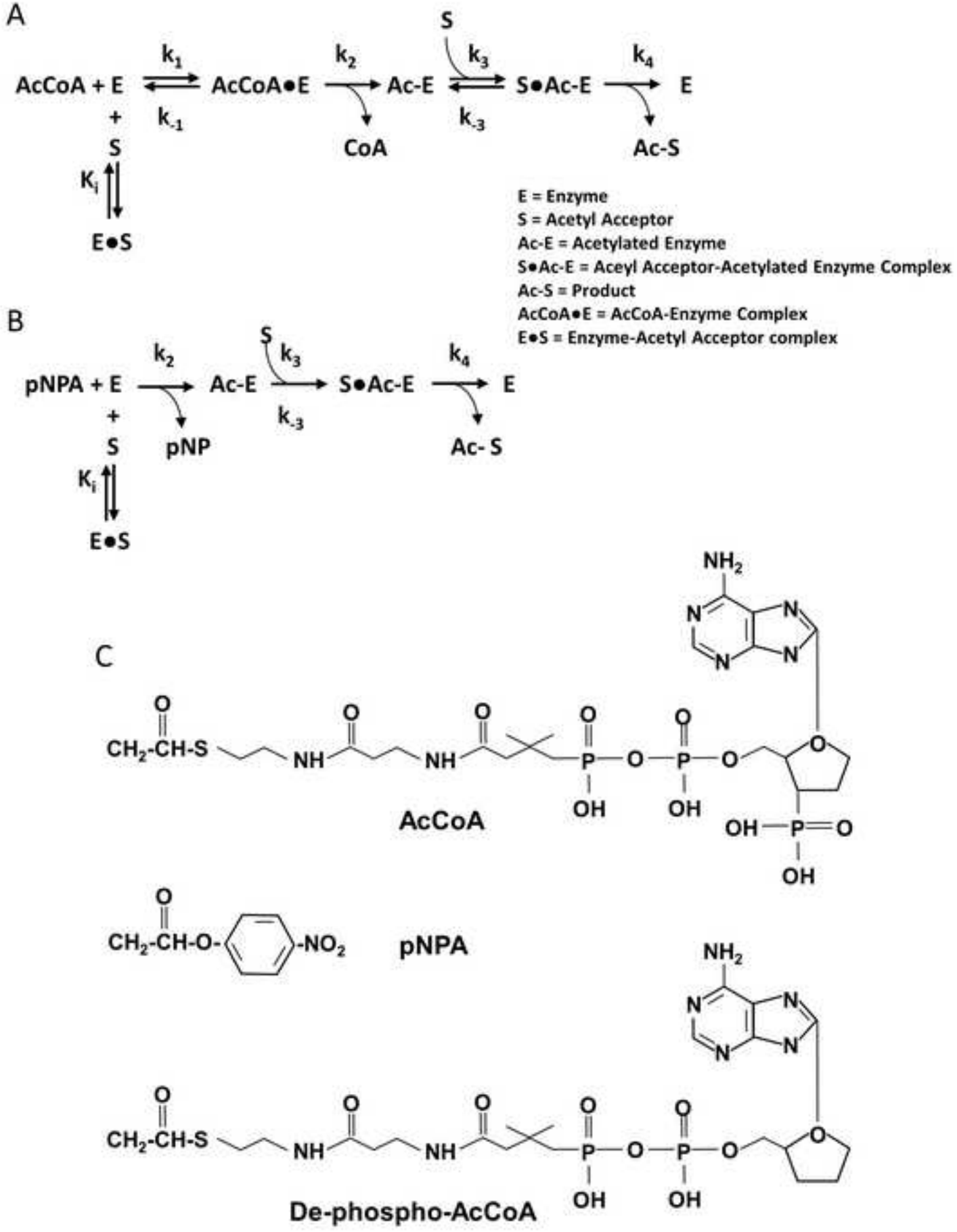

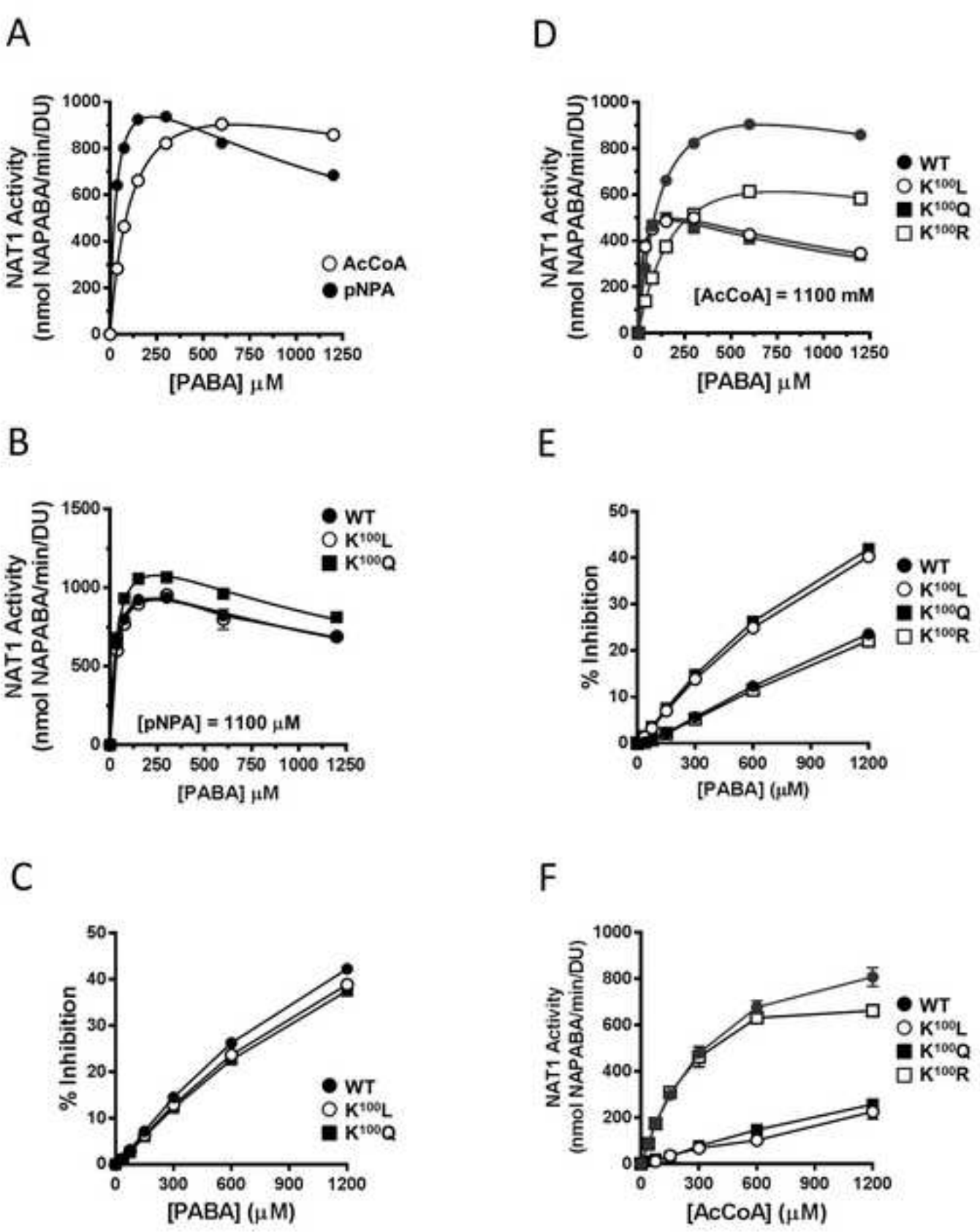

Figure 4

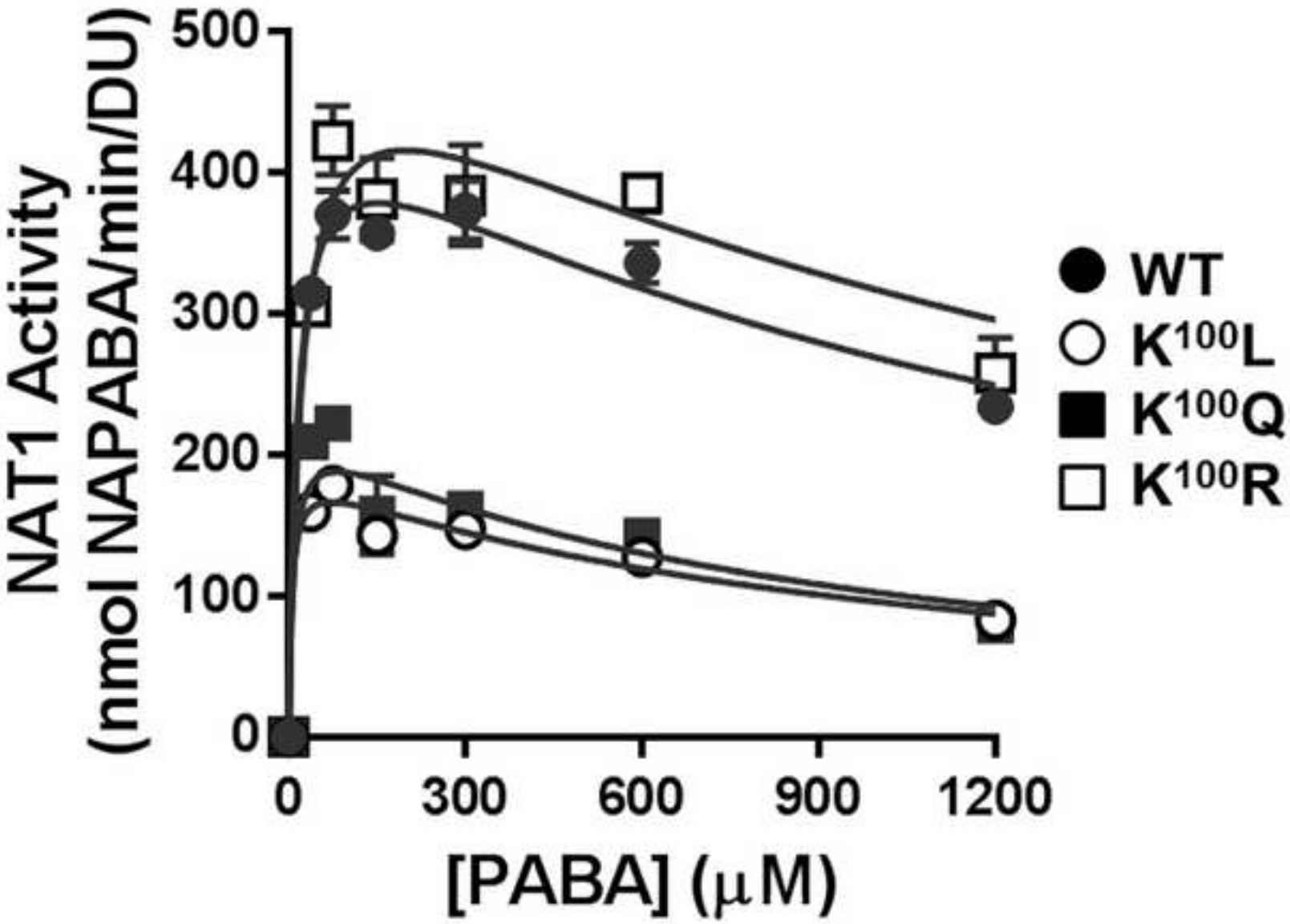
NAT1 Activity
(nmol NAPABA/min/DU)
500
400
300
200
100
0
0
300
600
900
1200
[PABA] (μM)
WT
K100L
K100Q
K100R